Published in Journal of Applied Physics, 117, 104510 -1/5, 2015
which should be used for any reference to this work

Demonstration of a high-performance pulsed optically pumped Rb clock based on a compact magnetron-type microwave cavity

S. Kang,[a] M. Gharavipour, C. Affolderbach, F.Gruet, and G. Mileti[b]
Laboratoire Temps-Fréquence (LTF), University of Neuchâtel, Neuchâtel 2000, Switzerland

We demonstrate a high-performance pulsed optically pumped (POP) Rb vapor-cell clock based on a magnetron-type microwave cavity of only 44 cm^3 external volume. Using optical detection, an unprecedented 35% contrast of the Ramsey signal has been obtained. Both the signal-to-noise ratio (of 30 000) and the estimated shot-noise limit of $1.7 \times 10^{-14}\ \tau^{-1/2}$ are at the same level as those found with a bigger cylindrical TE_{011} cavity (100 cm^3 inner volume) and are sufficient for achieving excellent clock stability. Rabi oscillations are measured and indicate a sufficiently uniform microwave magnetic field distribution inside the cavity. The instability sources for the POP clock's performance are analyzed. A short-term stability of $2.1 \times 10^{-13}\ \tau^{-1/2}$ is demonstrated which is consistent with the noise budget.

I. INTRODUCTION

Following its invention in late 1950s, and during 60-years of continuous development, the lamp-pumped[1] Rb clocks have been widely used in many industrial applications such as telecommunication, navigation, and space applications (e.g., GPS, GALILEO, and COMPASS)[2] because of their combined advantages of good frequency stability, compactness, reliability, and low power consumption. Further improvements on the stability of lamp-pumped Rb clocks are limited, in particular due to the discharge lamp's relatively low optical pumping efficiency. Laser-pumped Rb clocks[3–6] can achieve a better stability by at least one order of magnitude, and one of the most promising approaches is the pulsed optically pumped (POP) Rb clock with optical detection scheme.[7] While in the continuous-wave (CW) scheme opti-cal pumping, microwave interrogation and optical detection take place simultaneously, the POP scheme realizes these three phases separated in time. This allows achieving a higher signal-to-noise ratio (SNR) by individual optimization of the optical intensities for pumping and detection, and the suppression of the light shift (LS) effect.[8] Recently, a POP Rb clock prototype with a state-of-the-art stability of $1.6 \times 10^{-13}\ \tau^{-1/2}$ at 1s–10 000s timescales has been reported,[9] which is even better than that of a passive Hydrogen maser (PHM).[10] This previous POP work[9] used a Rb vapor cell of 20 mm diameter and length placed in cylin-drical TE_{011} microwave cavity[11] of ~100 cm^3 internal vol-ume. Here, we report a POP Rb clock demonstrator based on a slightly larger Rb vapor cell, but placed in a more compact 44 cm^3 volume magnetron-type microwave cavity.[12] This cavity has previously been applied in a Rb atomic clock based on CW interrogation,[13,14] but thanks to its uniform microwave magnetic field distribution, is also suitable for POP operation. Due to the much smaller size of the magnetron-type cavity, its implementation in a POP clock allows reducing the size of thermal and magnetic shields and thus enables a significant reduction in both volume and power consumption of the clock physics package, and eventually reduced temperature inhomogeneity. In the present article, we report on the POP clock's Ramsey signal, the homogeneity of the microwave field via observation of Rabi oscillations, and the POP clock's short-term stability performance.

II. POP Rb CLOCK SETUP

The schematic of our POP Rb clock prototype is shown in Fig. 1. Optical pumping (duration T_p) creates a significant atom population imbalance between the ^{87}Rb clock transition hyperfine energy levels ($5S_{1/2}$, F = 1, $m_F = 0$ t o 5 S $_{1/2}$, F = 2, $m_F = 0$). The laser beam is then switched off and interaction with two coherent $\pi/2$ microwave pulses (duration T_1) sepa-rated by a Ramsey time interval (duration T_{Ramsey}) probes the clock transition. Finally, a weaker optical detection pulse (duration T_d) produces a narrow clock-resonance Ramsey signal (linewidth ~ 100 Hz).

The core of our clock's physics package (PP) is the magnetron-type cavity whose resonant frequency is tuned to the ^{87}Rb clock's transition frequency (≈6.835 GHz), with a loaded quality factor of about 200. The cavity has an external diameter and length of 40 mm and 35 mm, respectively (total external volume: 44 cm^3) and holds a home-made 25 mm diameter vapor cell with enriched ^{87}Rb and a total 26 mbar of mixed buffer gas inside (Argon and Nitrogen, $P_{Ar}/P_{N2} = 1.6$). The vapor cell and the stem temperature are kept at 64 °C and 58 °C, respectively. The good homogeneity of the microwave magnetic field across the vapor cell volume makes the $\pi/2$ pulses sufficiently well realized for the majority of the atoms, to create a high contrast Ramsey signal. A telescope assembly in front of the cell expands the laser beam to ~19 mm diameter and a C-field coil creates a

[a]Permanent address: Key Laboratory of Atomic Frequency Standards, Chinese Academy of Sciences, Wuhan Institute of Physics and Mathematics, Wuhan 430071, China.
[b]Electronic mail: gaetano.mileti@unine.ch

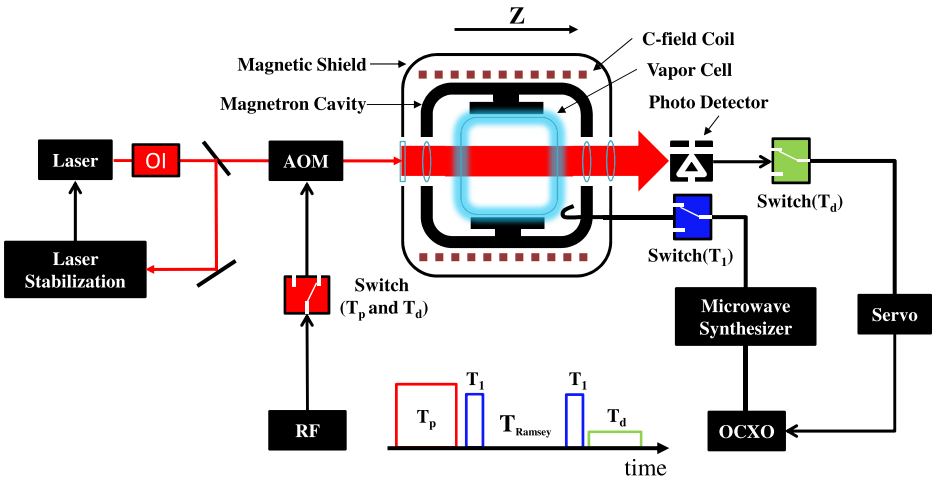

FIG. 1. Schematic setup of POP Rb clock with optical detection. T_P: Pumping time, T_1: Microwave pulse, T_{Ramsey}: Ramsey time, T_d: Detection time, and OI: Optical isolator.

~40 mG static magnetic field parallel to the laser propagation vector (Z direction). Behind the cell, a photo detector collects the transmitted light. A two-layer magnetic shield surrounds the whole PP to suppress external magnetic field fluctuations.

The laser source is a 780 nm distributed-feedback laser (DFB) frequency stabilized to the Doppler-free ^{87}Rb cross-over transition CO 1-01 ($F = 1$ to $F' = 0, 1$) from an auxiliary evacuated ^{87}Rb reference cell (10 mm diameter, 19 mm length). An acousto-optic modulator (AOM) driven by a 110 MHz radio frequency (RF) signal is used as an optical switch to control the durations and optical powers of optical pumping and detection pulses. The AOM also serves to detune the laser frequency by −110 MHz, thus close to the center of the optical transition in the Rb vapor cell (that is shifted by the presence of the buffer gas). The laser extinc-tion ratio during the Ramsey phase is 30 dB. The local oscil-lator (LO) is composed of the microwave synthesizer, the servo loop, and an oven-controlled crystal oscillator (OCXO) quartz oscillator.[15] The phase noise of the LO at 6.8 GHz that may limit the POP clock's stability through the well-known Dick effect,[16] is about −105 dBrad^2/Hz in the range from 100 Hz to 1000 Hz (at 6.8 GHz carrier).

III. EXPERIMENTAL RESULTS AND DISCUSSION

A. Ramsey fringes

During the pumping pulse ($T_P = 0.4$ ms) the laser power entering into the PP is set as high as possible (≈15 mW) to maximize the atomic ground-state population difference. The detection ($T_d = 0.5$ ms) laser power is set to about 100 μW, more than two orders of magnitude lower than the pumping power, to avoid re-pumping. The microwave power sent into the cavity and the pulse time (T_1) are about −20 dBm and 0.4 ms, respectively, for optimized Ramsey signal contrast. The Ramsey time (T_{Ramsey}) is 3 ms. Fig. 2 shows the experimental Ramsey fringes using the magnetron-type cavity, and the numerical simulation for the case of an ideal magnetic field (B_z totally homogeneous) running in $\pi/2$ pulse. The numerical simulations are carried out using the density matrix approach[17] and taking into account the other Zeeman sublevels in the ground state and an optical thick Rb vapor. In both cases, the central fringe's full width at half maximum (FWHM) is around 160 Hz (shown in the inset) and the cut-off frequencies (Δf) of the zero-order Rabi pedestal detuning from the clock transition frequency are about 2500 Hz. These values are consistent with the theoretical predictions (FWHM $= 1/2\ T_{Ramsey} \approx 167$ Hz and $\Delta f = 1/T_1 =$ 2500 Hz). The ideal field would produce a central fringe contrast up to 49% due to the fact that all the atoms in the cell undergo a $\pi/2$ pulse while the magnetron-type cavity gives a slightly lower contrast of 35% due to the residual microwave field inhomogeneity. 35% is, however, the high-est contrast reported to date for POP Rb clock with optical detection. The shot noise limit can be expressed as[9]

$$\sigma_{y,sn}(\tau) = \frac{1}{\pi Q_a R_{sn}} \sqrt{\frac{T_c}{\tau}}, \tag{1}$$

where Q_a is the quality factor of the clock transition ($\approx 4.3 \times 10^7$) and T_c is the cycle time ($=4.74$ ms). R_{sn} is the SNR defined as

$$R_{sn} = C\sqrt{\eta N_{opt}}, \tag{2}$$

where C is the central Ramsey fringe contrast and η is the efficiency of the photo detector. N_{opt} is the number of optical photons during the detection time T_d. For our magnetron-type cavity, R_{sn} is at a level of 30 000 and the expected shot-noise stability limit is $1.7 \times 10^{-14}\ \tau^{-1/2}$, both of which are

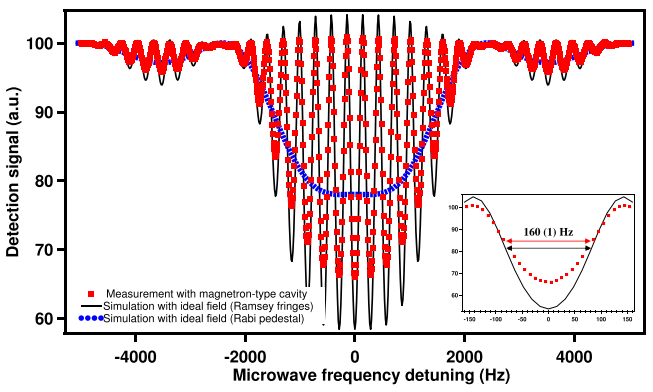

FIG. 2. Typical measured Ramsey pattern fringes based on the magnetron-type cavity (red squares) and simulation results for a hypothetical ideal field (solid black line, blue bullets show the Rabi pedestal). Inset: Central fringes.

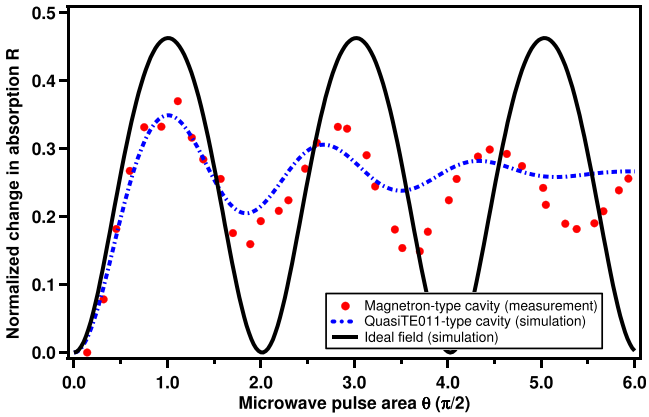

FIG. 3. Normalized change in optical absorption R as a function of microwave pulse area in units of $\pi/2$ for the magnetron-type cavity (experimental, red bullets), quasi TE_{011}-type cavity (simulation, blue dashed line), and ideal field (simulation, black solid line).

the same as those with the bigger cylindrical TE_{011} cavity.[9,18]

B. Rabi oscillation

Because in a buffer-gas cell the Rb atoms are subject to the local microwave magnetic field, the spatial homogeneity of the magnetic field (more specifically, of the B_z component driving the clock transition) over the vapor cell volume is of high importance for the Ramsey signal's contrast that will determine the POP clock's short-term frequency stability. In order to investigate the field distribution inside the magnetron-type cavity, we measured the normalized change in optical absorption R induced by the microwave pulse area (i.e., Rabi oscillations) when the microwave frequency is set to the center of the clock transition. Here, the normalized change in optical absorption R is defined as

$$R = 1 - I_t/I_0, \tag{3}$$

where I_t and I_0 are the transmitted detection pulse intensities for microwave pulse areas of θ and $\theta = 0$, respectively. For comparison, we simulated the Rabi oscillations for two other cavities' B_z distributions over the same cell volume: The ideal field distribution and a quasi TE_{011}-type cavity whose field distribution across the cell is expressed as

$$B_z^{quasiTE011}(r,\theta,z) = B_0 J_0\left(1.127\frac{r}{R}\right)\sin\left(\frac{\pi z}{L}\right),$$
$$0 \le r \le R,\ 0 \le z \le L, \tag{4}$$

where B_0 is the microwave magnetic field amplitude, R and L are the radius and length of the vapor cell, J_0 is the zero-order Bessel function, and the constant 1.127 is chosen to restrict the amplitude variation in radial (r) direction to the 30% of its maximum value demonstrated before.[19] The experimental and simulated results for R as a function of microwave pulse area (realized by varying the microwave power) are shown in Fig. 3. For convenient comparison of their evolution, we normalize the first-cycle's highest value of normalized change in optical absorption R for each cavity to occur at $\pi/2$ pulse area. As expected, the simulation result for the ideal field configuration shows an undamped oscilla-tion of R and each extremum position occurs at $\theta = n\cdot\pi/2$ (n is an integer) pulse. The quasi TE_{011}-type cavity, because of its residual B_z inhomogeneity, results in different atoms experiencing a range of pulse areas, and therefore shows a smaller oscillation amplitude with a damping, and a shift of extremum position for higher pulse areas. The experimental results for the magnetron-type cavity show intermediate per-formances on the amplitude, damping rate, and extremum position shift. It is clear that although not as good as the ideal field configuration, the magnetron-type cavity still has a more uniform B_z distribution than that in the quasi TE_{011}-type cavity, most likely due to its better homogeneity in the Z-direction.

C. Light-shift

In POP Rb clocks, the optical and microwave interrogation are separated in time and therefore the intensity and frequency LS can be considerably reduced compared to the CW scheme. The intensity LS coefficient α is defined as

$$\alpha = \frac{\delta v_{clock}}{\delta I_L}, \tag{5}$$

for a fixed laser frequency ν_L, with ν_{clock} as the clock frequency, and I_L as the laser intensity. The frequency LS coefficient β is defined as

$$\beta = \frac{\delta v_{clock}}{\delta v_L}, \tag{6}$$

for a given constant laser intensity I_L. Figs. 4(a) and 4(b) show the preliminary LS measurements for our POP Rb clock. At the clock working point (black dotted circle), the intensity light shift coefficient α is 5×10^{-14}/% and the

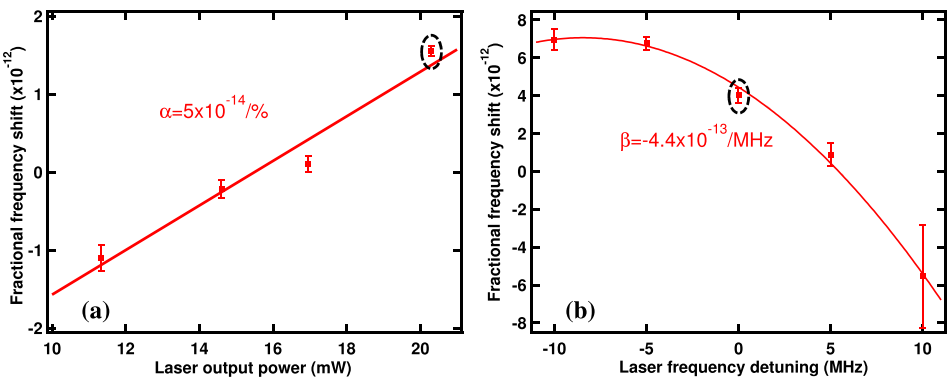

FIG. 4. POP Rb clock fractional frequency shift measured as a function of (a) laser's output power when laser frequency is locked to the sub-Doppler cross-over peaks CO 1-01 and AOM shifts the frequency −110 MHz and (b) laser frequency detuning from CO 1-01 plus −110 MHz shift when laser output power is fixed at 21 mW. The black dotted circle presents the final clock operating point.

TABLE I. POP Rb clock prototype's short-term stability budget.

Instability source	LS effect	Dick effect	Detection noise
$\sigma_y(\tau) \sim \tau^{-1/2}$	1×10^{-15}	7×10^{-14}	1.95×10^{-13}
Total		$2.07 \times 10^{-13}\ \tau^{-1/2}$	

frequency light shift coefficient β is -4.4×10^{-13}/MHz both of which are at least one order of magnitude lower than those observed in CW scheme.[13,14,20]

D. Short-term stability

The short-term stability of a POP Rb clock with optical detection can be simply expressed by

$$\sigma_y(\tau) = \sqrt{\sigma^2_{y,LS}(\tau) + \sigma^2_{y,Dick}(\tau) + \sigma^2_{y,\mathrm{det}}(\tau)}, \qquad (7)$$

where $\sigma_{y,\mathrm{LS}}(\tau)$ is the instability due to the intensity and frequency light shifts via the laser intensity noise and frequency instability on short-time scales. $\sigma_{y,\mathrm{Dick}}(\tau)$ is the contribution of local oscillator's phase noise through the Dick effect. $\sigma_{y,\mathrm{det}}(\tau)$ is the instability from the total optical detection noise which includes shot noise, laser's amplitude-modulation (AM) noise, AOM's additional AM noise and the noise from frequency-modulation (FM) noise (laser + AOM) to AM noise conversion in the vapor cell.[21] Table I presents the budget of the instability sources. The final expected stability limit is $2.07 \times 10^{-13}\ \tau^{-1/2}$ where the domi-nant contribution comes from the detection noise. Further analysis of the instability contribution for the detection noise is shown in Table II. The FM-to-AM noise is the major source of instability, similar to other high-performance vapor-cell clocks under study.[9,13,22] Additional AM noise from the AOM also introduces some non-negligible instabil-ity, mainly due to the RF signal's amplitude noise.

The present experimental short-term stability of POP Rb clock prototype is shown in Fig. 5. A numerical fitting gives a short-term stability of $2.1 \times 10^{-13}\ \tau^{-1/2}$, in good agreement with the predicted value. If the AOM's additional AM noise can be completely suppressed, the POP Rb clock would achieve a stability of $1.7 \times 10^{-13}\ \tau^{-1/2}$ which is very close to the best previously demonstrated vapor-cell clock stabilities.[4,9,13] Our POP clock prototype is still a relatively open setup, and its medium- to long-term performances are currently dominant by the temperature variation of cell's stem due to its enhanced temperature sensitivity (ETS).[23] However, the prototype's suppression of the light-shift effect is expected to reduce its light-shift stability limitation down to the level of 1×10^{-15} at the timescale of 10^4 s.[13]

TABLE II. Instability budget for the optical detection noise.

Noise source	Shot noise	AM (Laser)	AM (Laser + AOM)	FM-to-AM[a]
$\sigma_y(\tau) \sim \tau^{-1/2}$	1.7×10^{-14}	2.6×10^{-14}	1.21×10^{-13}	1.52×10^{-13}

[a]Laser's FM and AM noise (after AOM) are assumed to be uncorrelated here.

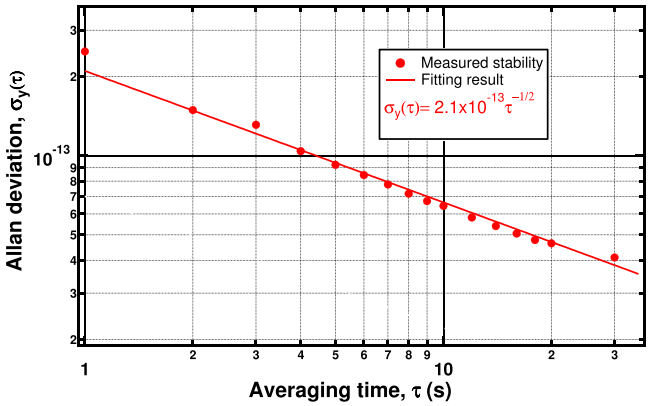

FIG. 5. Measured short-term stability of the POP Rb prototype.

IV. CONCLUSIONS

A good trade-off between the stability and compactness for the POP Rb clock based on the magnetron-type cavity has been demonstrated, while preserving the advantage of suppressed light shift. Based on a qualitative comparison of Rabi oscillations, the magnetron-type cavity demonstrates good uniformity of the microwave field across the vapor cell, suitable for POP operation. The POP Rb clock prototype achieves a Ramsey signal with high contrast of 35% with a linewidth of 160 Hz. Its shot-noise limit is estimated as $1.7 \times 10^{-14}\ \tau^{-1/2}$, comparable to that obtained with a much larger TE_{011} cavity. The measured stability of $2.1 \times 10^{-13}\ \tau^{-1/2}$ agrees with the theoretical estimations. The short-term stability budget shows that FM-to-AM noise conversion and the AOM's additional AM noise account for the dominant instability contribution. Suppression of optical detection AM noise would allow a short-term stability of $1.7 \times 10^{-13}\ \tau^{-1/2}$, and with further improvements even below $1.0 \times 10^{-13}\ \tau^{-1/2}$ can be feasible. Such a compact high-performance Rb clock could find applications in industrial applications, such as telecommunication, navigation, and space applications. Our results also show that a high quality factor of the microwave cavity is not necessarily required for the realization of a vapor-cell POP clock with state-of-the art stability performance: The very moderate quality factor of 200 of our magnetron-type cavity is sufficient for operating our POP clock and is highly desirable for achieving low instability contributions due to the cavity pulling effect.[24]

ACKNOWLEDGMENTS

This work was supported by the Swiss National Science Foundation (SNSF Grant No. 140712) and the European Metrology Research Programme (EMRP Project IND55-Mclocks). The EMRP is jointly funded by the EMRP participating countries within EURAMET and the European Union. We also acknowledge previous support from the European Space Agency (ESA) and the Swiss Space Office (Swiss Confederation). We thank A. K. Skrivervik, C. Stefanucci (both EPFL-LEMA) and M. Pellaton and T. Bandi (both UniNe-LTF) for their contributions to realizing the cell and cavity and C. Calosso (INRIM, Italy) for providing the LO.

[1]A. Kastler, J. Opt. Soc. Am. **47**, 460 (1957).
[2]L. A. Mallette, J. White, and P. Rochat, "Space qualified frequency sources (clocks) for current and future GNSS applications 2010," in *Position Location and Navigation Symposium* (2010), pp. 903–908.
[3]J. C. Camparo and R. P. Frueholz, J. Appl. Phys. **59**, 3313 (1986).
[4]G. Mileti, J. Q. Deng, F. L. Walls, D. A. Jennings, and R. E. Drullinger, IEEE J. Quantum Electron. **34**, 233 (1998).
[5]J. Vanier, Appl. Phys. B **81**, 421 (2005).
[6]J. Vanier and C. Mandache, Appl. Phys. B **87**, 565 (2007).
[7]S. Micalizio, A. Godone, F. Levi, and C. E. Calosso, Phys. Rev. A **79**, 013403 (2009).
[8]B. S. Mathur, H. Tang, and W. Happer, Phys. Rev. **171**, 11 (1968).
[9]S. Micalizio, C. E. Calosso, A. Godone, and F. Levi, Metrologia **49**, 425 (2012).
[10]F. Droz, P. Mosset, Q. Wang, P. Rochat, M. Belloni, M. Gioia, A. Resti, and P. Waller, "Space passive hydrogen maser – performances and lifetime data," in *Proceedings of Joint International Frequency Control Symposium (IFCS) and European Frequency and Time Forum (EFTF)* (2009), pp. 393–398.
[11]A. Godone, S. Micalizio, F. Levi, and C. Calosso, Rev. Sci. Instrum. **82**, 074703 (2011).
[12]C. Stefanucci, T. Bandi, F. Merli, M. Pellaton, C. Affolderbach, G. Mileti, and A. K. Skrivervik, Rev. Sci. Instrum. **83**, 104706 (2012).
[13]T. Bandi, C. Affolderbach, C. Stefanucci, F. Merli, A. K. Skrivervik, and G. Mileti, IEEE Trans. Ultrason., Ferroelectr., Freq. Control **61**, 1769 (2014).
[14]T. Bandi, C. Affolderbach, C. E. Calosso, and G. Mileti, Electron. Lett. **47**, 698 (2011).
[15]C. E. Calosso, S. Micalizio, A. Godone, E. K. Bertacco, and F. Levi, IEEE Trans. Ultrason., Ferroelectr., Freq. Control **54**, 1731 (2007).
[16]G. J. Dick, "Local oscillator induced instabilities in trapped ion frequency standards," in *Proceedings of Precise Time and Time Interval* (1987), pp. 133–147.
[17]S. Micalizio, C. E. Calosso, F. Levi, and A. Godone, Phys. Rev. A **88**, 033401 (2013).
[18]S. Kang, C. Affolderbach, F. Gruet, M. Gharavipour, C. E. Calosso, and G. Mileti, "Pulsed optical pumping in a Rb vapor cell using a compact magnetron-type microwave cavity," in *Proceedings of 26th European Frequency and Time Forum (EFTF)* (2014), pp. 544–547.
[19]A. Ivanov, T. Bandi, G. X. Du, A. Horsley, C. Affolderbach, P. Treutlein, G. Mileti, and A. K. Skrivervik, "Experimental and numerical study of the microwave field distribution in a compact magnetron-type microwave cavity," in *Proceedings of 26th European Frequency and Time Forum (EFTF)* (2014), pp. 208–211.
[20]T. Bandi, C. Affolderbach, and G. Mileti, J. Appl. Phys. **111**, 124906 (2012).
[21]J. C. Camparo, J. Opt. Soc. Am. B **15**, 1177 (1998).
[22]J.-M. Danet, O. Kozlova, P. Yun, S. Gu´erandel, and E. de Clercq, Eur. Phys. J. Web Conf. **77**, 00017 (2014).
[23]C. E. Calosso, A. Godone, F. Levi, and S. Micalizio, IEEE Trans. Ultrason., Ferroelectr., Freq. Control **59**, 2646 (2012).
[24]J. Vanier and C. Audoin, *The Quantum Physics of Atomic Frequency Standards* (Adam Hilger, Bristol, UK, 1989).